Monoallelic BMP2 Variants Predicted to Result in Haploinsufficiency Cause Craniofacial, Skeletal, and Cardiac Features Overlapping Those of 20p12 Deletions

Tan, Tiong Yang ; Gonzaga-Jauregui, Claudia ; Bhoj, Elizabeth J ; et al ; Steindl, Katharina ; Joset, Pascal ; Rauch, Anita

Abstract: Bone morphogenetic protein 2 (BMP2) in chromosomal region 20p12 belongs to a gene superfamily encoding TGF- -signaling proteins involved in bone and cartilage biology. Monoallelic deletions of 20p12 are variably associated with cleft palate, short stature, and developmental delay. Here, we report a cranioskeletal phenotype due to monoallelic truncating and frameshift BMP2 variants and deletions in 12 individuals from eight unrelated families that share features of short stature, a recognizable craniofacial gestalt, skeletal anomalies, and congenital heart disease. De novo occurrence and autosomal-dominant inheritance of variants, including paternal mosaicism in two affected sisters who inherited a BMP2 splice-altering variant, were observed across all reported families. Additionally, we observed similarity to the human phenotype of short stature and skeletal anomalies in a heterozygous Bmp2-knockout mouse model, suggesting that haploinsufficiency of BMP2 could be the primary phenotypic determinant in individuals with predicted truncating variants and deletions encompassing BMP2. These findings demonstrate the important role of BMP2 in human craniofacial, skeletal, and cardiac development and confirm that individuals heterozygous for BMP2 truncating sequence variants or deletions display a consistent distinct phenotype characterized by short stature and skeletal and cardiac anomalies without neurological deficits.

DOI: https://doi.org/10.1016/j.ajhg.2017.10.006

Monoallelic *BMP2* Variants Predicted to Result in Haploinsufficiency Cause Craniofacial, Skeletal, and Cardiac Features Overlapping Those of 20p12 Deletions

Tiong Yang Tan,[1,2,3,*] Claudia Gonzaga-Jauregui,[4] Elizabeth J. Bhoj,[5] Kevin A. Strauss,[6] Karlla Brigatti,[6] Erik Puffenberger,[6] Dong Li,[5] LiQin Xie,[7] Nanditha Das,[7] Ioanna Skubas,[7] Ron A. Deckelbaum,[7] Virginia Hughes,[7] Susannah Brydges,[7] Sarah Hatsell,[7] Chia-Jen Siao,[7] Melissa G. Dominguez,[7] Aris Economides,[7] John D. Overton,[4] Valerie Mayne,[8] Peter J. Simm,[2,3,8] Bryn O. Jones,[2,8] Stefanie Eggers,[2] Gwenaël Le Guyader,[9] Fanny Pelluard,[10] Tobias B. Haack,[11] Marc Sturm,[11] Angelika Riess,[11] Stephan Waldmueller,[11,12] Michael Hofbeck,[12] Katharina Steindl,[13] Pascal Joset,[13] Anita Rauch,[13] Hakon Hakonarson,[5] Naomi L. Baker,[2,3] and Peter G. Farlie[2,3]

Bone morphogenetic protein 2 (*BMP2*) in chromosomal region 20p12 belongs to a gene superfamily encoding TGF-β-signaling proteins involved in bone and cartilage biology. Monoallelic deletions of 20p12 are variably associated with cleft palate, short stature, and developmental delay. Here, we report a cranioskeletal phenotype due to monoallelic truncating and frameshift *BMP2* variants and deletions in 12 individuals from eight unrelated families that share features of short stature, a recognizable craniofacial gestalt, skeletal anomalies, and congenital heart disease. *De novo* occurrence and autosomal-dominant inheritance of variants, including paternal mosaicism in two affected sisters who inherited a *BMP2* splice-altering variant, were observed across all reported families. Additionally, we observed similarity to the human phenotype of short stature and skeletal anomalies in a heterozygous *Bmp2*-knockout mouse model, suggesting that haploinsufficiency of BMP2 could be the primary phenotypic determinant in individuals with predicted truncating variants and deletions encompassing *BMP2*. These findings demonstrate the important role of *BMP2* in human craniofacial, skeletal, and cardiac development and confirm that individuals heterozygous for *BMP2* truncating sequence variants or deletions display a consistent distinct phenotype characterized by short stature and skeletal and cardiac anomalies without neurological deficits.

Bone morphogenetic proteins (BMPs), so named for their osteogenic function,[1] belong to the TGF-β superfamily of secreted signaling proteins, which are involved in diverse biological processes. There are over 15 BMP ligands and two subtypes of transmembrane serine/threonine protein kinase receptors that multimerize and phosphorylate downstream SMAD transcription modulators to transduce the BMP signal to the nucleus for the purpose of regulating target genes.[2] BMPs play important roles in the development of the musculoskeletal system, most prominently bone and cartilage. They have additional functions in body-plan patterning[3] and the development of other organs, including the eyes[4] and heart.[5] Endochondral ossification, the primary mechanism of bone formation in mammals, requires mesenchymal condensation and differentiation into chondrocytes to form the cartilage template to be replaced by bone. In animal models, *Bmp2* mRNA transcripts have been detected in these pre-chondrogenic mesenchymal condensations and hypertrophic cartilage of long bones.[6] These chondrocytes express *Bmp2* and *Bmp6*,[7] and functional redundancy of these two molecules in the regulation of bone formation has been demonstrated in compound-knockout mice.[8] *Bmp2*-null mice show embryonic lethality with failure of amnion and chorion formation and abnormal cardiac development, whereas heterozygous mice have been reported to be phenotypically normal.[9]

Human disorders linked to dysfunctional BMP signaling are characterized by chondrodysplasia,[10,11] skeletal and ocular malformations,[12,13] brachydactyly,[14–16] abnormal joint formation,[17,18] and heterotopic ossification.[19] Human *BMP2* (MIM: 112261) is located in chromosomal region 20p12,[20] and variably sized monoallelic deletions involving this locus have been reported in association with short stature, structural and electrophysiologic cardiac anomalies, cleft palate, distinctive facial features (including a long philtrum), Pierre Robin sequence (MIM: 261800), hearing impairment, and development delay.[21–24] In three previously reported individuals, *BMP2* was the only deleted gene.[21,22] The phenotypes of other reported individuals have been complicated by the involvement of multiple genes such as *JAG1* (MIM: 601920)[22,23] or

[1]Victorian Clinical Genetics Services, Melbourne, VIC 3052, Australia; [2]Murdoch Children's Research Institute, Melbourne, VIC 3052, Australia; [3]Department of Paediatrics, University of Melbourne, Melbourne, VIC 3052, Australia; [4]Regeneron Genetics Center, Regeneron Pharmaceuticals Inc., Tarrytown, NY 10591, USA; [5]Center for Applied Genomics, Department of Pediatrics, Children's Hospital of Philadelphia, Philadelphia, PA 19104-4399, USA; [6]Clinic for Special Children, Philadelphia, PA 17579, USA; [7]Regeneron Pharmaceuticals Inc., Tarrytown, NY 10591, USA; [8]Royal Children's Hospital, Parkville, Melbourne, VIC 3052, Australia; [9]Department of Medical Genetics, Poitiers University Hospital, Poitiers 86021, France; [10]Department of Pathology, Bordeaux University Hospital, Bordeaux 33076, France; [11]Institute of Medical Genetics and Applied Genomics, University of Tuebingen, 72076 Tuebingen, Germany; [12]Universitätsklinik für Kinder- und Jugendmedizin, Kinderheilkunde II Kardiologie Intensivmedizin Pulmologie, 72076 Tuebingen, Germany; [13]Institute of Medical Genetics, University of Zurich, 8952 Schlieren-Zurich, Switzerland
*Correspondence: tiong.tan@vcgs.org.au
https://doi.org/10.1016/j.ajhg.2017.10.006.

other chromosomal anomalies.[23] Microduplications of non-coding DNA containing putative regulatory elements approximately 110 kb downstream of *BMP2* have been found in individuals with brachydactyly type A2 (MIM: 112600), an autosomal-dominant phenotype characterized by malformations of the middle phalanx of the index finger and abnormalities of the second toe.[25,26]

Herein, we report on 12 individuals from eight families affected by *de novo* or inherited monoallelic *BMP2* sequence variants and deletions associated with a phenotype characterized by short stature, palatal anomalies, congenital heart disease or arrhythmia, and skeletal malformations. Additionally, we demonstrated paternal mosaicism for a splice-site variant in one family with two affected sisters born to an unaffected mosaic parent and identified two families with a parentally inherited interstitial 20p12 deletion involving *BMP2*. We propose that the clinical overlap between individuals with *BMP2* truncating sequence variants and 20p12 deletions is suggestive of haploinsufficiency as the primary phenotypic determinant.

All Australian individuals (families 1–3 and individual S1 from family 4) were identified from cohorts of children with short stature or with syndromic non-isolated cleft palate and Pierre Robin sequence.[27,28] Contact between international collaborators was facilitated by the European Society of Human Genetics annual meeting and the use of GeneMatcher, a web-based tool for connecting researchers with an interest in the same gene.[29] Informed written consent was obtained from all participating individuals and their parents according to local institutional requirements and approved protocols. Clinical details of all affected individuals were collected in PhenoTips[30] with standardized Human Phenotype Ontology[31] terms. Research exome sequencing (of individuals F1-1, F1-2, S2, S3, and S4) or chromosomal microarray (of individuals F3-1, F3-2, F8-1, and F8-2 and probands from the other families) were undertaken as previously described.[32–35] Individuals F2-1 and S1 were sequenced by a custom-designed Agilent SureSelect craniofacial panel comprising 79 genes and the non-coding region upstream of *SOX9* (MIM: 608160). Library preparation was performed according to the manufacturer's instructions. Sequencing was performed on a Illumina MiSeq sequencer with 2× 150 bp reads, and Fastq files were analyzed by Cpipe 2.1.[36] Sanger sequencing was performed to validate all sequence variants in probands and first-degree relatives. Bone mineral density was assessed with a Horizon-W Dual Energy X-Ray Absorptiometry (DXA) scanner (Hologic). *Z* scores were calculated with the use of age- and sex-specific normative data provided by Hologic, and height matching was based on the reference dataset from the Bone Mineral Density in Childhood Study.[37]

Clinical phenotypes of all affected individuals are summarized in Table 1 and detailed in Table S1 and the Supplemental Note. Affected individuals share similar distinctive craniofacial features such as a broad forehead with temporal narrowing, a flat midface, anteverted nares, a long philtrum, a thin upper lip, crowded dentition, and a cleft or high-arched palate (Figures 1A–1H and 1A′–1H′). Skeletal anomalies include proportionate short stature, short fifth proximal phalanges, 11 pairs of ribs, and a wide sandal gap (Figures 1I–1M). Phalangeal anomalies were observed in affected individuals and most commonly involved the fifth finger through shortening of the proximal phalanx or clinodactyly (Table S1). Cardiac malformations were reported in 4/9 (44.4%) individuals and included Ebstein anomaly, transposition of the great arteries, ventricular septal defects, and pulmonary valve stenosis. Cardiac arrhythmias (Wolff-Parkinson-White syndrome, paroxysmal supraventricular tachycardia, and non-specific palpitations) were reported in 3/9 (33.3%) individuals. Less common features noted in at least two individuals were conductive hearing impairment, low-set posteriorly rotated ears, synophrys, sternal deformity, delayed bone age in early childhood, and L5/S1 spondylolisthesis. Three individuals (F2-1, S1, and S4) had Pierre Robin sequence and a cleft palate, and two of them required mandibular distraction osteogenesis. Four individuals (F2-1, F2-2, S1, and S3) had obstructive sleep apnea diagnosed in childhood or adulthood. All individuals have normal cognitive development, although hypotonia in infancy was observed in three individuals. All individuals who had previously had biochemical studies such as calcium, phosphate, alkaline phosphatase, or parathyroid hormone levels showed normal results. Bone densitometry was normal for height in all affected children. However, individual F3-2, the father of F3-1, was found to have generalized osteopenia at age 54 years but no history of fracture. The other two adults (individuals F2-2 and F8-1) have not undergone bone densitometry studies. All *BMP2* genomic lesions and their inheritance are listed in Table 2 and depicted diagrammatically in Figure 1. All sequence variants identified are predicted to result in a truncated protein and are absent from public population databases, such as the ExAC Browser, gnomAD, the NHLBI Exome Sequencing Project (ESP) Exome Variant Server, 1000 Genomes, and internal institutional databases.

Individuals F1-1 and F1-2 are affected sisters born to clinically unaffected parents. Their father had a history of Wilms tumor as a child, for which he had standard therapy. He is 167.1 cm tall and has a normal palate and no cardiac murmur. Although the pedigree of family 1 suggested an autosomal-recessive mode of inheritance, we considered nonsynonymous, splice-altering, and frameshift variants under either *de novo* dominant or recessive inheritance models with a minor allele frequency $< 1\%$ in population databases. Subsequent gene prioritization was based on deleteriousness prediction and biological and clinical relevance. Exome sequencing of individual F1-1 yielded 567 nonsynonymous, splice-altering, and frameshift variants that matched dominant, X-linked, or recessive models after a standard filtering strategy. Among these, a splice-altering variant, c.−7−2_−7−1delAGinsCC,

Table 1. Clinical Characteristics of Affected Individuals with *BMP2* Variants and Deletions

Demographics	Affected Individuals	
	Total	Percentage
Gender	6 male, 6 female	–
Growth		
Gestation < 37 weeks	1/9	11.1%
Birth weight ≤ −2.0 SD	1/9	11.1%
Birth length ≤ −2.0 SD	1/7	14.3%
Birth head circumference ≤ −2.0 SD	0/7	0.0%
Weight ≤ −2.0 SD	4/9	44.4%
Height ≤ −2.0 SD[a]	8/11	72.7%
Head circumference ≤ −2.0 SD	2/8	25.0%
Craniofacial		
Broad forehead[a]	8/12	66.7%
Temporal narrowing[a]	8/10	80.0%
Synophrys[a]	5/9	55.6%
Downslanting palpebral fissures	3/12	25.0%
Midface hypoplasia[a]	11/12	91.7%
Low-set, posteriorly rotated ears[a]	7/12	58.3%
Short nose[a]	12/12	100.0%
Anteverted nares[a]	12/12	100.0%
Long philtrum[a]	12/12	100.0%
Thin upper lip[a]	10/12	83.3%
Everted lower-lip vermilion	2/7	28.6%
Palatal anomaly[a]	11/11	100.0%
Pierre Robin sequence	3/11	27.3%
Dental		
Dental crowding[a]	6/10	60.0%
Anterior open bite[a]	5/10	50.0%
Airway		
Airway malacia	1/11	9.1%
Obstructive sleep apnea	4/11	36.4%
Skeletal		
11 pairs of ribs[a]	6/9	66.7%
Sternal deformity	4/11	36.4%
L5/S1 spondylolisthesis	3/9	33.3%
Vertebral defect	2/9	22.2%
Limited pronation and supination	2/11	18.2%
Phalangeal abnormalities[a]	10/10	100.0%
Fifth-finger clinodactyly	4/11	36.4%
Single palmar crease	2/11	18.2%
Sandal gap[a]	8/11	72.7%
Toenail dysplasia	3/11	27.3%
Delayed bone age	2/5	40.0%
Cardiac		
Congenital heart disease	4/9	44.4%
Arrhythmia	3/9	33.3%
Other		
Conductive hearing impairment	4/11	36.4%
Normal intellect[a]	11/11	100.0%
Hypotonia	3/11	27.3%
Normal bone biochemistry[a]	8/8	100.0%
Osteopenia on bone densitometry	1/6	16.7%

[a]These features were observed in 50% or more of affected individuals. Note that denominators vary depending on the availability of data.

which deletes AG and inserts CC at the splice acceptor site of intron 1 in the 5′ UTR of *BMP2* (GenBank: NM_001200.3), was selected as a candidate causative variant because of its association with the TGF-β signaling pathway and bone biology. Subsequent Sanger sequencing identified the splice acceptor variant in both affected children, but both parents were found to be wild-type. We exome sequenced parental DNA to identify possible mosaicism not detectable by Sanger sequencing; however, we did not observe any mutant alleles in 57 reads to suggest mosaicism in DNA from parental blood samples. Alternate paternity was excluded through shared SNP analysis of the father and children. After parental exome data were available, we reanalyzed the trio, and no viable recessive candidate variants remained. To facilitate identification of *de novo* dominant or gonadal mosaic variants, we presumed that the variants responsible for the condition would be rare and probably absent in the general population. Therefore, we filtered for variants not present in the 1000 Genomes Project and not identified in control subjects by our in-house exome variant database; this approach resulted in one additional candidate, c.4148C>G (p.Thr1383Arg) in *ABCA7* (MIM: 605414), which encodes an ATP-binding cassette transporter protein that primarily moves lipids across membranes and has been shown to mediate phagocytosis.[38] Approximately 100 variants in *ABCA7* have been reported to be significantly associated with Alzheimer disease,[38,39] and studies suggest a role in amyloid production as a

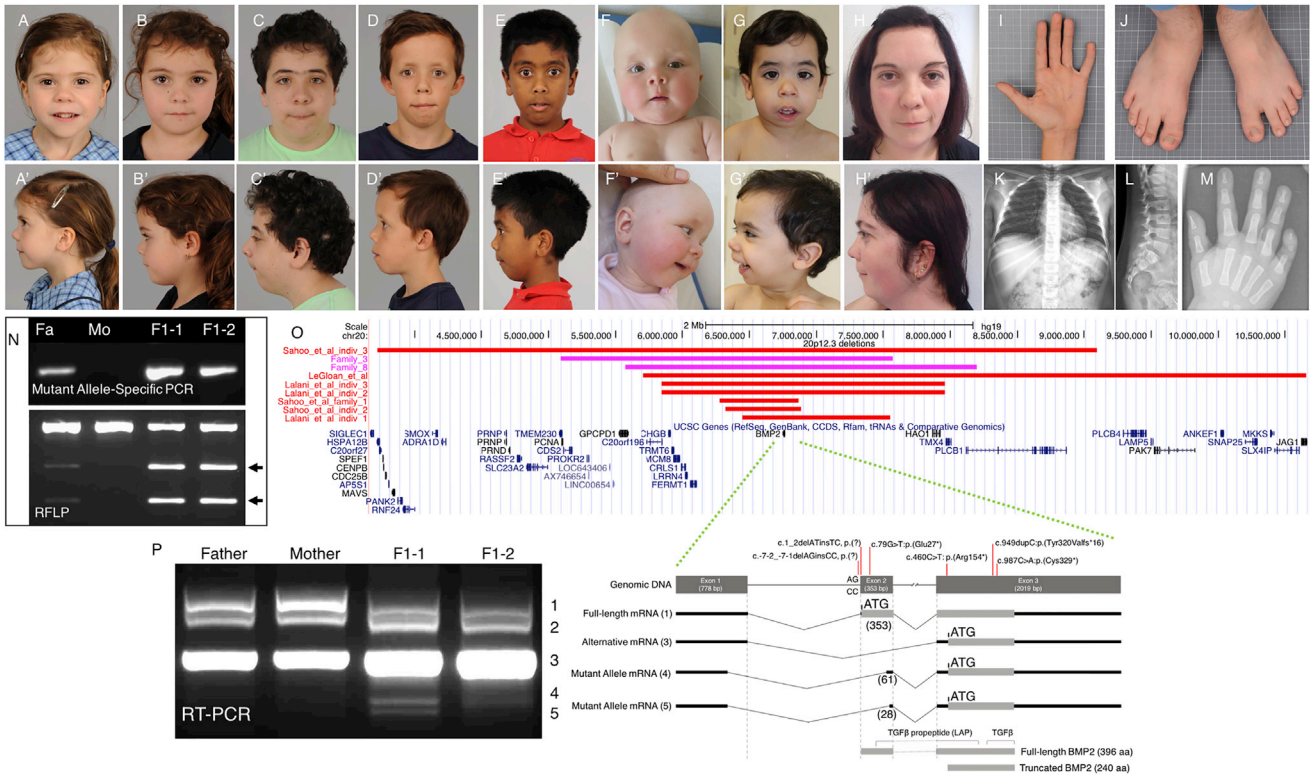

Figure 1. Clinical Phenotype of Affected Individuals and Demonstration of Mosaicism and Splicing Alterations in Family 1
(A–F) Frontal and lateral views of the craniofacial features of individual F1-1 (A and A′), individual F1-2 (B and B′), individual F2-1 (C and C′), individual F3-1 (D and D′), individual S1 (E and E′), individual S3 (F and F′), individual S4 (G and G′), and individual F8-1 (H and H′). Note the short upturned nose, flat midface, long philtrum, micrognathia, and low-set posteriorly rotated ears, as well as the pectus excavatum in individual S3 (F).
(I–M) Skeletal phenotypes. Note the fifth-finger clinodactyly (I), wide sandal gap (J), 11 pairs of ribs (K), L5/S1 spondylolisthesis (L), and short fifth middle phalanx and distal phalanges (M).
(N) Mutant-allele specific PCR demonstrates mosaicism (top), such that an amplicon was detected in both affected children and their unaffected father. Mosaicism was confirmed by RFLP (bottom). EciI digestion of amplified *BMP2* resulted in two smaller fragments in both affected children and their unaffected father (arrows).
(O) The two 20p12 deletions involving *BMP2* identified in families 3 and 8 in our cohort, as well as the seven previously reported deletions (some of the breakpoints are approximated from individual reports[21–23]).
(P) RT-PCR analysis of *BMP2* mRNA in family 1 (left) and the positions of all genomic sequence variants and the various splicing outcomes (right). The *BMP2* splice-site variant results in multiple mRNA products (1–5). Product 1 is the full-length *BMP2* mRNA, product 3 is the *BMP2* X1 alternate transcript, and product 2 is a heteroduplex of products 1 and 3. Products 4 and 5 result from apparent activation of two cryptic splice sites. Each truncated mRNA (products 3–5) is predicted to result in a 240 aa truncated BMP2.

contributing factor in Alzheimer disease susceptibility.[40] Although residue Thr1383 is located in a highly conserved region and was predicted to be damaging with high probability by prediction algorithms SIFT and PolyPhen-2 (0 and 0.97, respectively), we considered that the *ABCA7* substitution was a less likely candidate for a cranioskeletal phenotype. In contrast, *BMP2* is strongly associated with skeletal development, and the splice variant was absent from large population databases including the 1000 Genomes Project, COSMIC v.80, ESP6500SI, and gnomAD and data from more than 4,000 samples that we had previously exome sequenced in our in-house database.

To further investigate the possibility of gonosomal mosaicism in the ostensibly unaffected parents of individuals F1-1 and F1-2, we extracted DNA from buccal cells and lymphoblasts from both parents and from a paternal urine sample. Mutant-allele-specific PCR (forward primer 5′-CG TCGGTCCTGTCCGCCC-3′ and reverse primer 5′-GGAA GCTGCGCACAGTGTTG-3′) identified the familial *BMP2* variant in all three genomic samples from the father, confirming somatic mosaicism (Figure 1N, top). No PCR product was amplified from any of the mother's genomic samples. To confirm mosaicism in the unaffected father in family 1, we designed a restriction fragment length polymorphism (RFLP) assay given that the variant introduces a novel EciI restriction site. Analysis of digested PCR products further confirmed the presence of the mutation in the two children and their father (mosaic) and its absence in the mother (Figure 1N, bottom).

The c.−7−2_−7−1delAGinsCC variant is predicted to disrupt the *BMP2* intron 1 splice acceptor, resulting in the production of a truncated mRNA lacking part of exon 2 (first coding exon). To confirm this, we performed RT-PCR analysis of lymphoblast total RNA by using primers spanning

Table 2. Summary of *BMP2* Variants and Deletions and Inheritance Patterns in All Affected Individuals

Family	Individual	Method	Deletion Coordinates (hg19)	Nucleotide Change (GenBank: NM_001200.3)	Predicted Amino Acid Change	Inheritance
1	individuals F1-1 (proband) and F1-2 (sister)	exome sequencing	normal microarray	c.−7−2_−7−1delAGinsCC	p.?	familial; paternal mosaicism
2	individuals F2-1 (proband) and F2-2 (mother)	custom capture Agilent SureSelect panel	normal microarray	c.79G>T	p.Glu27*	familial; maternal
3	individuals F3-1 (proband) and F3-2 (father)	chromosome microarray	chr20: 5,089,999–7, 566,496	not applicable	not applicable	familial; paternal
4	individual S1	custom capture Agilent SureSelect panel	normal microarray	c.1_2delATinsTC	p.?	most likely sporadic; not maternal
5	individual S2	exome sequencing	normal microarray	c.949dupC	p.Tyr320Valfs*16	sporadic; *de novo*
6	individual S3	exome sequencing	normal microarray	c.987C>A	p.Cys329*	sporadic; *de novo*
7	individual S4	exome sequencing	normal microarray	c.460C>T	p.Arg154*	sporadic; *de novo*
8	individuals F8-1 (proband) and F8-2 (fetus)	chromosome microarray	chr20: 5,572,697–8, 196,643	not applicable	not applicable	familial; maternal (*de novo* in proband)

the c.−7−2_−7−1delAGinsCC variant (a forward primer in exon 1 [5′-AGAATAACTTGCGCACCCCA-3′] and a reverse primer in exon 3 [5′-CCACTTCCACCACGAATCCA-3′]). The three products amplified in both parents included a full-length *BMP2* amplicon (band 1), a truncated product missing exon 2 (band 3, *BMP2*, GenBank: NM_001200.3 transcript variant X1), and a heteroduplex of bands 1 and 3 (band 2). All resulting amplicons in the father and F1-1 were gel extracted and sequenced, allowing us to determine the various splice events. The heteroduplex band was also gel extracted and sequenced, allowing us to read the two alleles. These three products, as well as two additional smaller amplicons that most likely result from activation of cryptic splice sites within exon 2, were also amplified in both children. Sanger sequencing of gel-purified PCR products revealed that band 4 contained 61 nucleotides of exon 2, whereas band 5 contained only 28 nucleotides from exon 2 (Figure 1P).

Given that all *BMP2* variants identified in human individuals were predicted to be truncating and result in haploinsufficiency, we re-derived and phenotyped heterozygous *Bmp2*-knockout mice previously generated as part of the Knockout Mouse Project.[41] *Bmp2*$^{+/-}$ mice were generated by the VelociGene method.[42,43] All experiments were performed in accordance with the Institutional Animal Care and Use Committee (IACUC) of Regeneron Pharmaceuticals according to IACUC-approved protocols. Coding exon 1 was deleted beginning just after the start ATG to the end of coding exon 1, leaving the last 4 bp, and was replaced with a *lacZ* reporter cassette containing a neomycin resistance gene under the control of the human *UBC* (ubiquitin [MIM: 191340]) promoter (Figure S1). For assessment of endogenous tissue expression, the cassette was cloned such that the *lacZ* coding sequence was in frame with the mouse *Bmp2* start codon. Consistent with previous reports, homozygous *Bmp2*-knockout mice died before embryonic day 12.5 (E12.5). Expression analysis of the *Bmp2-lacZ* reporter in heterozygous E12.5 embryos showed specific and strong staining in vibrissae follicles, the facial dermis, the supraorbital dermis, Meckel's cartilage, and the embryonic dental epithelium that gives rise to ameloblasts (Figures S2A–S2D), consistent with dental anomalies and distinctive facial features in individuals with *BMP2* mutations. We further observed strong expression in the cartilaginous primordia of the appendicular and axial skeleton (limb and ribs; Figures S2E–S2G) and in the developing heart (valves and ventricular-atrial junctions; Figures S2F–S2H), consistent with the gene's demonstrated role and importance in skeletal and cardiac development.

We performed computed tomography (μCT) scans of *Bmp2*$^{+/-}$ mice at 10 weeks to correlate with the skeletal phenotypes observed in human individuals, mainly abnormal numbers of rib pairs (Figures 2A–2D) and short stature (Figures 2E–2J). Of the 13 *Bmp2*$^{+/-}$ mice evaluated, 10 mice had 12 pairs of ribs and were missing the 13th rib pair at thoracic vertebral 13 (T13) (Figures 2D1 and 2D2); the remaining three mice had 12.5 pairs and were missing one rib unilaterally (Figures 2C1 and 2C2). None of the 13 scanned wild-type littermates were found to have rib abnormalities (Figures 2B1 and 2B2). We measured the distance from the snout to the base of the tail (at caudal vertebra 4), as well as femur and tibia lengths, of *Bmp2*$^{+/-}$ mice and their wild-type littermates (Figure S3). We observed that the body of heterozygous *Bmp2* mice was significantly shorter than that of wild-type mice, consistent with short stature in human individuals, but the two groups of mice showed no differences in femur or tibia length (Figures 2E–2G). Pixi and μCT data showed that *Bmp2*$^{+/-}$ mice had significantly less bone mineral content and volume than wild-type mice (Figures 2H–2J). Because of the significant bone mineral content and reduced bone volume in *Bmp2*$^{+/-}$ mice, we performed three-point bending flexural tests to evaluate the

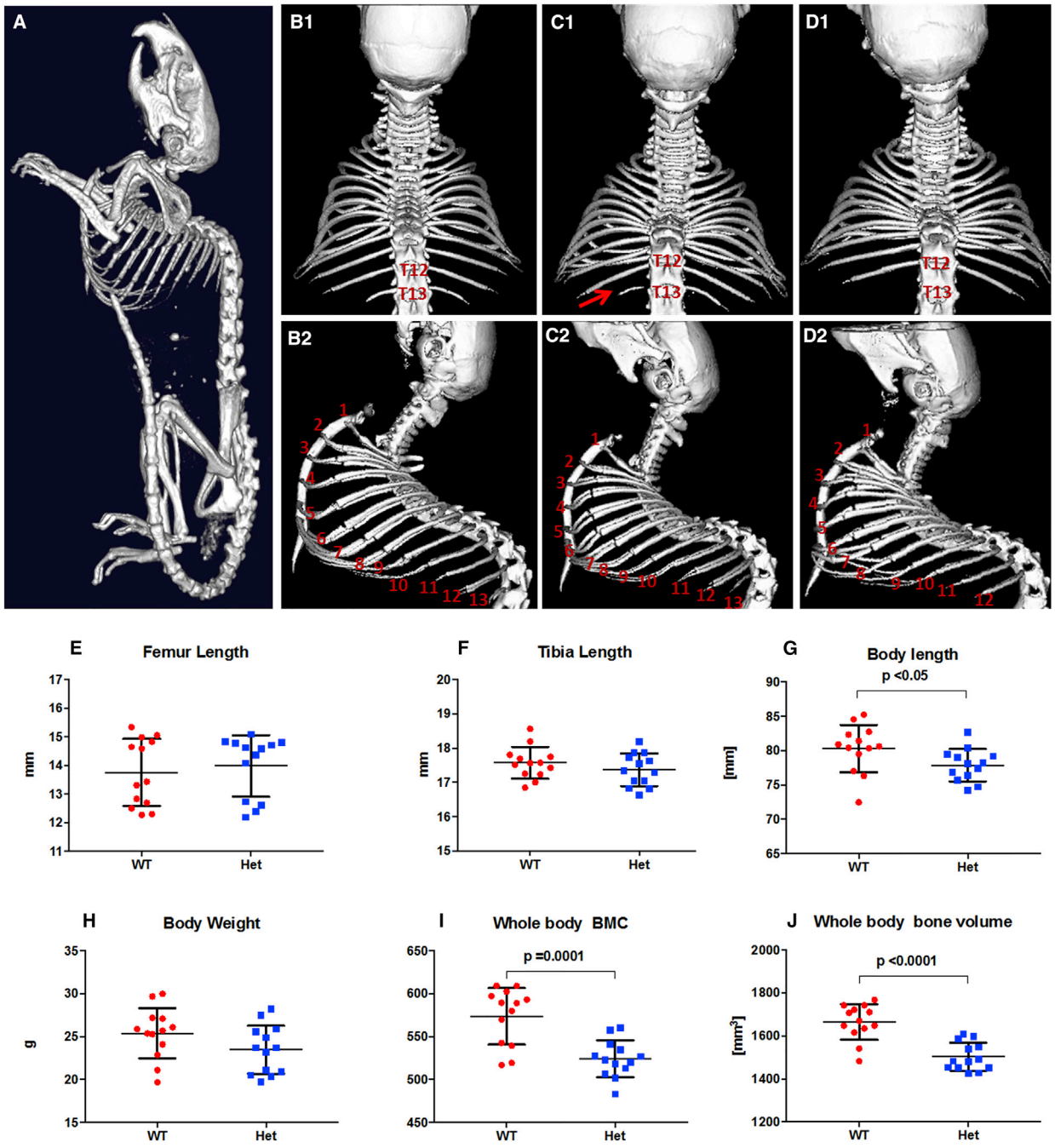

Figure 2. Computed Tomography (μCT) Scans and Quantification of Skeletal Phenotypes Observed in *Bmp2*$^{+/-}$ and Wild-Type Mice

Heterozygous *Bmp2*$^{+/-}$ mice (n = 13) and wild-type (WT) littermates (n = 13) were scanned *in vivo* at 10 weeks for evaluation of their skeletal phenotype.

(A) Sagittal view of a full-body scan of a WT mouse for reference.

(B1 and B2) Coronal (B1) and sagittal (B2) views of a WT mouse show a normal number of rib pairs (13). All WT mice evaluated had a normal number of rib pairs.

(C1 and C2) Coronal (C1) and sagittal (C2) views of one of three (3/13) *Bmp2*$^{+/-}$ mice that showed 12.5 rib pairs, including the unilateral absence or presence of a smaller floating rib (red arrow).

(D1 and D2) Coronal (D1) and sagittal (D2) views of one of ten (10/13) *Bmp2*$^{+/-}$ mice that showed a complete absence of a rib pair at thoracic vertebrae 13 (T13), consistent with the phenotype observed in humans.

(E–G) Femur length (E), tibia length (F), and total body length from the snout to the base of the tail (G) were measured from μCT scans of *Bmp2*$^{+/-}$ mice and WT littermates evaluated at 10 weeks of age (Figure S2). No significant differences were observed in femur and tibia lengths between *Bmp2*$^{+/-}$ and WT mice; however, heterozygous mice showed a significantly shorter body length, consistent with the short stature in affected humans.

(H–J) Whole-body weight (H), bone mineral content (BMC) (I), and bone volume (J) were assessed through μCT and Pixi data. A trend toward reduced body weight in the heterozygous *Bmp2*$^{+/-}$ mice was observed, but this was not significant. Whole-body BMC and volume were significantly lower in *Bmp2*$^{+/-}$ mice than in WT littermates.

mechanical properties of the femoral bones in heterozygous and wild-type mice. We did not observe any significant differences in maximum load, yield load, work to failure, or stiffness between the two groups (data not shown).

Although the contribution of genetics to human stature is well established with an estimated heritability of 80%–90%, it is generally considered a polygenic trait with quantitatively small and variable contribution from multiple loci. Genome-wide association studies have identified a multitude of potentially contributing loci that all together account for about a fifth of height heritability.[44] However, ascertainment and genetic analyses of individuals and families in whom reduced stature segregates significantly have unveiled several genes that have large effects on human linear growth when mutated.[45] Many of these growth disorders are often accompanied by additional features, such as skeletal abnormalities and distinct craniofacial features or other organ defects, implicating these genes in broader human development beyond their functions in bone formation and skeletogenesis. BMPs, and TGF-β signaling more broadly, have been extensively studied in vertebrate development and human disease. *Bmp2* is known to be important in skeletal, craniofacial (including dental), and cardiac development, and tissue expression patterns are consistent with this.[6] The individuals reported herein demonstrate a human phenotype associated with monoallelic sequence variants and deletions possibly resulting in *BMP2* haploinsufficiency, as well as malformations also affecting these same systems. Although we have not experimentally demonstrated that any of the alleles leads to nonsense-mediated decay, all sequence variants are predicted to result in a truncated and probably non-functional BMP2. Although the phenotype is recognizable, it can be mild, as demonstrated by the variability between the affected sisters in family 1 and the normal stature in individual S1. The craniofacial features—midface retrusion, a short upturned nose, a long philtrum, a high-arched or cleft palate, and variable degrees of micrognathia and dental crowding—are distinctive. The observation of Pierre Robin sequence in three individuals could shed important insights into the pathogenesis of mandibular hypoplasia and cleft palate in non-syndromic patients and is consistent with its previous association with chondrogenic defects.[46] *BMP2* should also be considered a candidate gene in individuals with Pierre Robin sequence and short stature. The skeletal phenotype involves patterning defects of the axial skeleton (11 pairs of ribs) and brachydactyly, especially affecting the fifth ray, such that radiographic anomalies of the middle and distal phalanges are commonly observed, consistent with previous observations of digital abnormalities associated with BMP signaling dysfunction.[11,14–16,25,47] Although the *Bmp2*-haploinsufficient mouse was initially reported as phenotypically normal,[9] we observed a similar, highly penetrant loss of the caudal-most rib in $Bmp2^{+/-}$ mice. This phenotype has also been observed in mice homozygous for a hypomorphic *Bmpr2* allele resulting in the posterior transformation of the final thoracic vertebra into a lumbar vertebra and the loss of a rib pair.[5] It has been proposed that anteroposterior patterning of the spine could be sensitive to relative levels of BMP and TGF-β and activin signaling.[5] In addition, our detailed phenotypic analysis of the heterozygous knockout mice identified a decrease in bone mineral content and volume at 12 postnatal weeks and a reduction in overall body length. The short stature of affected individuals in this cohort is consistent with the shorter body length of $Bmp2^{+/-}$ mice; however, unlike the relative truncal shortening in mice, no skeletal disproportion was observed in affected humans.

Assessment of bone mineral density in five children revealed normal height-adjusted lumbar spine bone mineral density (from −0.5 to 0.5 SD), and one adult demonstrated generalized osteopenia at age 54 years but no significant history of fracture. This is interesting also in the context of the mouse evaluation, where no significant differences in the mechanical properties of femurs were observed, despite the significant differences in bone content. These results suggest that although bone composition is different in $Bmp2^{+/-}$ mice, their bones are not more prone to breakage or fracture than those of wild-type mice. Longitudinal studies will be necessary for determining whether a clinically significant reduction in bone density occurs in affected adults. Although BMP2 has been applied in the orthopedic field for fracture repair,[48,49] our study opens additional potential therapeutic avenues for study.

Individuals from families 3 (F3-1 and F3-2) and 8 (F8-1 and F8-2) were found to have overlapping 2.5–2.6 Mb microdeletions involving *BMP2* and surrounding genes. Notably, previously published individuals with deletions have had a variable spectrum of developmental delay, generally attributed to the concomitant deletion of surrounding genes. A previously reported individual with a 1.1 Mb deletion involving *BMP2* alone displayed only mild developmental delay.[22] Individual F3-1 and his father (F3-2) and individual F8-1 are intellectually normal despite the deletion of additional genes surrounding *BMP2*, suggesting that these genes do not play a major role in cognitive development. Given that individuals with truncating variants in *BMP2* do not have any neurocognitive deficits, it is unlikely that monoallelic loss of *BMP2* is the cause of the neurodevelopmental concerns reported in individuals with larger 20p12 deletions. Besides the cognitive phenotype, the observation that individuals with *BMP2* sequence variants predicted to result in reduced amounts of BMP2 are clinically indistinguishable from those with a microdeletion involving *BMP2* suggests that the primary craniofacial, skeletal, and cardiac phenotypic determinant in all individuals reported here could be haploinsufficiency of *BMP2*. Moreover, the overlap between features of the human phenotype and those of the heterozygous knockout mouse model further supports that haploinsufficiency of

BMP2 is the main driver of the short stature and skeletal abnormalities observed in human individuals.

Additional features variably observed in human individuals, such as congenital heart defects, mandibular and tooth abnormalities, and distinctive craniofacial features, correlate well with the specific endogenous expression of mouse *Bmp2* in the corresponding tissues during murine embryonic development, as observed by lacZ staining in our animal model. Interestingly, the congenital heart disease observed in individuals F1-1, S1, and S2 involved the cardiac outflow tract (transposition of the great arteries, pulmonary valve stenosis, and Ebstein anomaly). Mice with reduced *Bmp2* signaling due to a hypomorphic *Bmpr2* allele also demonstrated defects of the cardiac outflow tract,[48,49] whereas conditional deletion of *Bmp2* in the atrioventricular myocardium resulted in failure to form atrioventricular cushions and abnormal myocardial patterning.[50] Although investigation of *BMP2*-related SNPs found no association with congenital heart disease in humans,[51] data from mouse models highly suggest a causative role for *BMP2* haploinsufficiency in the cardiac phenotypes observed in the individuals reported herein. The diagnosis of cardiac arrhythmia in individuals S3 and S4 is in keeping with previously reported individuals with 20p12 deletions[22,23] and confirms the association.

The obstructive sleep apnea diagnosed in four individuals (including F2-2, the mother of F2-1) is most likely related to their craniofacial changes and is an important consideration in the longitudinal medical care of other affected individuals.

Together, our findings of individuals with *BMP2* truncating sequence variants and deletions associated with craniofacial, skeletal, and cardiac phenotypes and the related skeletal phenotypes observed in $Bmp2^{+/-}$ mice strongly support a role for *BMP2* in the etiology of a distinct cranioskeletal syndrome. On the basis of our data, we hypothesize that haploinsufficiency is the likely underlying mechanism, although we cannot exclude alternative explanations. Even though it is difficult to draw robust genotype-phenotype correlations in a small cohort of 12 individuals, large population datasets such as gnomAD are relatively devoid of loss-of-function alleles in *BMP2*, and further research could elucidate the functional consequences of missense mutations in this gene. These findings extend our understanding of *BMP2* biology and highlight the dosage-sensitive nature of this pathway. *BMP2* haploinsufficiency can join the growing list of rare but highly penetrant Mendelian growth disorders, adding to our understanding of the genes and pathways that contribute to skeletal patterning, development, and human linear growth.

Supplemental Data

Supplemental Data include a Supplemental Note, three figures, and one table and can be found with this article online at https://doi.org/10.1016/j.ajhg.2017.10.006.

Conflicts of Interest

C.G.-J., L.X., N.D., I.S., R.A.D., V.H., S.B., S.H., C.-J.S., M.G.D., A.E., and J.D.O. are full-time employees of Regeneron Pharmaceuticals Inc. and receive stock options as part of compensation.

Acknowledgments

The authors thank the affected individuals and all family members for participating in this research. This research was supported by an internal grant from the Murdoch Children's Research Institute Cell Biology Theme. The Murdoch Children's Research Institute receives funding from the Victorian State Government through the Operational Infrastructure Support Program. A.R. was supported by radiz – Rare Disease Initiative Zürich, the Clinical Research Priority Program for Rare Diseases at the University of Zurich. We thank Bernard Drew, Trent Burgess, Juliane Gohlke, and Beate Kootz for technical support.

Received: August 4, 2017
Accepted: October 11, 2017
Published: November 30, 2017

Web Resources

1000 Genomes, http://www.internationalgenome.org
ClinVar, https://www.ncbi.nlm.nih.gov/clinvar/
ExAC Browser, http://exac.broadinstitute.org
GenBank, https://www.ncbi.nlm.nih.gov/genbank/
GeneMatcher, https://genematcher.org/
GitHub, https://github.com
gnomAD, http://gnomad.broadinstitute.org/
NHLBI Exome Sequencing Project (ESP) Exome Variant Server, http://evs.gs.washington.edu/EVS/UCSC
OMIM, http://www.omim.org
Genome Browser, https://genome.ucsc.edu

References

1. Urist, M.R. (1965). Bone: formation by autoinduction. Science *150*, 893–899.
2. Massagué, J., and Wotton, D. (2000). Transcriptional control by the TGF-beta/Smad signaling system. EMBO J. *19*, 1745–1754.
3. Meinhardt, H. (2015). Dorsoventral patterning by the Chordin-BMP pathway: a unified model from a pattern-formation perspective for Drosophila, vertebrates, sea urchins and Nematostella. Dev. Biol. *405*, 137–148.
4. Furuta, Y., and Hogan, B.L. (1998). BMP4 is essential for lens induction in the mouse embryo. Genes Dev. *12*, 3764–3775.
5. Délot, E.C., Bahamonde, M.E., Zhao, M., and Lyons, K.M. (2003). BMP signaling is required for septation of the outflow tract of the mammalian heart. Development *130*, 209–220.
6. Lyons, K.M., Pelton, R.W., and Hogan, B.L. (1990). Organogenesis and pattern formation in the mouse: RNA distribution patterns suggest a role for bone morphogenetic protein-2A (BMP-2A). Development *109*, 833–844.
7. Chung, U.I., Schipani, E., McMahon, A.P., and Kronenberg, H.M. (2001). Indian hedgehog couples chondrogenesis to osteogenesis in endochondral bone development. J. Clin. Invest. *107*, 295–304.

8. Kugimiya, F., Kawaguchi, H., Kamekura, S., Chikuda, H., Ohba, S., Yano, F., Ogata, N., Katagiri, T., Harada, Y., Azuma, Y., et al. (2005). Involvement of endogenous bone morphogenetic protein (BMP) 2 and BMP6 in bone formation. J. Biol. Chem. *280*, 35704–35712.
9. Zhang, H., and Bradley, A. (1996). Mice deficient for BMP2 are nonviable and have defects in amnion/chorion and cardiac development. Development *122*, 2977–2986.
10. Thomas, J.T., Lin, K., Nandedkar, M., Camargo, M., Cervenka, J., and Luyten, F.P. (1996). A human chondrodysplasia due to a mutation in a TGF-beta superfamily member. Nat. Genet. *12*, 315–317.
11. Demirhan, O., Türkmen, S., Schwabe, G.C., Soyupak, S., Akgül, E., Tastemir, D., Karahan, D., Mundlos, S., and Lehmann, K. (2005). A homozygous BMPR1B mutation causes a new subtype of acromesomelic chondrodysplasia with genital anomalies. J. Med. Genet. *42*, 314–317.
12. Bakrania, P., Efthymiou, M., Klein, J.C., Salt, A., Bunyan, D.J., Wyatt, A., Ponting, C.P., Martin, A., Williams, S., Lindley, V., et al. (2008). Mutations in BMP4 cause eye, brain, and digit developmental anomalies: overlap between the BMP4 and hedgehog signaling pathways. Am. J. Hum. Genet. *82*, 304–319.
13. Ye, M., Berry-Wynne, K.M., Asai-Coakwell, M., Sundaresan, P., Footz, T., French, C.R., Abitbol, M., Fleisch, V.C., Corbett, N., Allison, W.T., et al. (2010). Mutation of the bone morphogenetic protein GDF3 causes ocular and skeletal anomalies. Hum. Mol. Genet. *19*, 287–298.
14. Lehmann, K., Seemann, P., Silan, F., Goecke, T.O., Irgang, S., Kjaer, K.W., Kjaergaard, S., Mahoney, M.J., Morlot, S., Reissner, C., et al. (2007). A new subtype of brachydactyly type B caused by point mutations in the bone morphogenetic protein antagonist NOGGIN. Am. J. Hum. Genet. *81*, 388–396.
15. Lehmann, K., Seemann, P., Stricker, S., Sammar, M., Meyer, B., Süring, K., Majewski, F., Tinschert, S., Grzeschik, K.H., Müller, D., et al. (2003). Mutations in bone morphogenetic protein receptor 1B cause brachydactyly type A2. Proc. Natl. Acad. Sci. USA *100*, 12277–12282.
16. Seemann, P., Schwappacher, R., Kjaer, K.W., Krakow, D., Lehmann, K., Dawson, K., Stricker, S., Pohl, J., Plöger, F., Staub, E., et al. (2005). Activating and deactivating mutations in the receptor interaction site of GDF5 cause symphalangism or brachydactyly type A2. J. Clin. Invest. *115*, 2373–2381.
17. Gong, Y., Krakow, D., Marcelino, J., Wilkin, D., Chitayat, D., Babul-Hirji, R., Hudgins, L., Cremers, C.W., Cremers, F.P., Brunner, H.G., et al. (1999). Heterozygous mutations in the gene encoding noggin affect human joint morphogenesis. Nat. Genet. *21*, 302–304.
18. Dawson, K., Seeman, P., Sebald, E., King, L., Edwards, M., Williams, J., 3rd, Mundlos, S., and Krakow, D. (2006). GDF5 is a second locus for multiple-synostosis syndrome. Am. J. Hum. Genet. *78*, 708–712.
19. Shore, E.M., Xu, M., Feldman, G.J., Fenstermacher, D.A., Cho, T.J., Choi, I.H., Connor, J.M., Delai, P., Glaser, D.L., LeMerrer, M., et al. (2006). A recurrent mutation in the BMP type I receptor ACVR1 causes inherited and sporadic fibrodysplasia ossificans progressiva. Nat. Genet. *38*, 525–527.
20. Rao, V.V., Löffler, C., Wozney, J.M., and Hansmann, I. (1992). The gene for bone morphogenetic protein 2A (BMP2A) is localized to human chromosome 20p12 by radioactive and nonradioactive in situ hybridization. Hum. Genet. *90*, 299–302.
21. Sahoo, T., Theisen, A., Sanchez-Lara, P.A., Marble, M., Schweitzer, D.N., Torchia, B.S., Lamb, A.N., Bejjani, B.A., Shaffer, L.G., and Lacassie, Y. (2011). Microdeletion 20p12.3 involving BMP2 contributes to syndromic forms of cleft palate. Am. J. Med. Genet. A. *155A*, 1646–1653.
22. Lalani, S.R., Thakuria, J.V., Cox, G.F., Wang, X., Bi, W., Bray, M.S., Shaw, C., Cheung, S.W., Chinault, A.C., Boggs, B.A., et al. (2009). 20p12.3 microdeletion predisposes to Wolff-Parkinson-White syndrome with variable neurocognitive deficits. J. Med. Genet. *46*, 168–175.
23. Le Gloan, L., Pichon, O., Isidor, B., Boceno, M., Rival, J.M., David, A., and Le Caignec, C. (2008). A 8.26Mb deletion in 6q16 and a 4.95Mb deletion in 20p12 including JAG1 and BMP2 in a patient with Alagille syndrome and Wolff-Parkinson-White syndrome. Eur. J. Med. Genet. *51*, 651–657.
24. Williams, E.S., Uhas, K.A., Bunke, B.P., Garber, K.B., and Martin, C.L. (2012). Cleft palate in a multigenerational family with a microdeletion of 20p12.3 involving BMP2. Am. J. Med. Genet. A. *158A*, 2616–2620.
25. Dathe, K., Kjaer, K.W., Brehm, A., Meinecke, P., Nürnberg, P., Neto, J.C., Brunoni, D., Tommerup, N., Ott, C.E., Klopocki, E., et al. (2009). Duplications involving a conserved regulatory element downstream of BMP2 are associated with brachydactyly type A2. Am. J. Hum. Genet. *84*, 483–492.
26. Su, P., Ding, H., Huang, D., Zhou, Y., Huang, W., Zhong, L., Vyse, T.J., and Wang, Y. (2011). A 4.6 kb genomic duplication on 20p12.2-12.3 is associated with brachydactyly type A2 in a Chinese family. J. Med. Genet. *48*, 312–316.
27. Tan, T.Y., Amor, D.J., Riley, M., Halliday, J., Kilpatrick, N., Simms, K., and White, S.M. (2009). Registry- and clinic-based analyses of birth defects and syndromes associated with cleft lip/palate in Victoria, Australia. Cleft Palate Craniofac. J. *46*, 583–587.
28. Xu, J.X., Kilpatrick, N., Baker, N.L., Penington, A., Farlie, P.G., and Tan, T.Y. (2016). Clinical and Molecular Characterisation of Children with Pierre Robin Sequence and Additional Anomalies. Mol. Syndromol. *7*, 322–328.
29. Sobreira, N., Schiettecatte, F., Valle, D., and Hamosh, A. (2015). GeneMatcher: a matching tool for connecting investigators with an interest in the same gene. Hum. Mutat. *36*, 928–930.
30. Girdea, M., Dumitriu, S., Fiume, M., Bowdin, S., Boycott, K.M., Chénier, S., Chitayat, D., Faghfoury, H., Meyn, M.S., Ray, P.N., et al. (2013). PhenoTips: patient phenotyping software for clinical and research use. Hum. Mutat. *34*, 1057–1065.
31. Groza, T., Köhler, S., Moldenhauer, D., Vasilevsky, N., Baynam, G., Zemojtel, T., Schriml, L.M., Kibbe, W.A., Schofield, P.N., Beck, T., et al. (2015). The Human Phenotype Ontology: Semantic Unification of Common and Rare Disease. Am. J. Hum. Genet. *97*, 111–124.
32. Hackenberg, A., Baumer, A., Sticht, H., Schmitt, B., Kroell-Seger, J., Wille, D., Joset, P., Papuc, S., Rauch, A., and Plecko, B. (2014). Infantile epileptic encephalopathy, transient choreoathetotic movements, and hypersomnia due to a De Novo missense mutation in the SCN2A gene. Neuropediatrics *45*, 261–264.
33. Li, D., Yuan, H., Ortiz-Gonzalez, X.R., Marsh, E.D., Tian, L., McCormick, E.M., Kosobucki, G.J., Chen, W., Schulien, A.J., Chiavacci, R., et al. (2016). GRIN2D Recurrent De Novo Dominant Mutation Causes a Severe Epileptic Encephalopathy Treatable with NMDA Receptor Channel Blockers. Am. J. Hum. Genet. *99*, 802–816.
34. Strauss, K.A., Gonzaga-Jauregui, C., Brigatti, K.W., Williams, K.B., King, A.K., Van Hout, C., Robinson, D.L., Young, M.,

Praveen, K., Heaps, A.D., et al. (2017). Genomic diagnostics within a medically underserved population: efficacy and implications. Genet. Med. Published online July 20, 2017. https://doi.org/10.1038/gim.2017.76.
35. Bruno, D.L., Ganesamoorthy, D., Schoumans, J., Bankier, A., Coman, D., Delatycki, M., Gardner, R.J., Hunter, M., James, P.A., Kannu, P., et al. (2009). Detection of cryptic pathogenic copy number variations and constitutional loss of heterozygosity using high resolution SNP microarray analysis in 117 patients referred for cytogenetic analysis and impact on clinical practice. J. Med. Genet. *46*, 123–131.
36. Sadedin, S.P., Dashnow, H., James, P.A., Bahlo, M., Bauer, D.C., Lonie, A., Lunke, S., Macciocca, I., Ross, J.P., Siemering, K.R., et al.; Melbourne Genomics Health Alliance (2015). Cpipe: a shared variant detection pipeline designed for diagnostic settings. Genome Med. *7*, 68.
37. Kalkwarf, H.J., Gilsanz, V., Lappe, J.M., Oberfield, S., Shepherd, J.A., Hangartner, T.N., Huang, X., Frederick, M.M., Winer, K.K., and Zemel, B.S. (2010). Tracking of bone mass and density during childhood and adolescence. J. Clin. Endocrinol. Metab. *95*, 1690–1698.
38. Steinberg, S., Stefansson, H., Jonsson, T., Johannsdottir, H., Ingason, A., Helgason, H., Sulem, P., Magnusson, O.T., Gudjonsson, S.A., Unnsteinsdottir, U., et al.; DemGene (2015). Loss-of-function variants in ABCA7 confer risk of Alzheimer's disease. Nat. Genet. *47*, 445–447.
39. Stenson, P.D., Mort, M., Ball, E.V., Howells, K., Phillips, A.D., Thomas, N.S., and Cooper, D.N. (2009). The Human Gene Mutation Database: 2008 update. Genome Med. *1*, 13.
40. Satoh, K., Abe-Dohmae, S., Yokoyama, S., St George-Hyslop, P., and Fraser, P.E. (2015). ATP-binding cassette transporter A7 (ABCA7) loss of function alters Alzheimer amyloid processing. J. Biol. Chem. *290*, 24152–24165.
41. Lloyd, K.C. (2011). A knockout mouse resource for the biomedical research community. Ann. N Y Acad. Sci. *1245*, 24–26.
42. Poueymirou, W.T., Auerbach, W., Frendewey, D., Hickey, J.F., Escaravage, J.M., Esau, L., Doré, A.T., Stevens, S., Adams, N.C., Dominguez, M.G., et al. (2007). F0 generation mice fully derived from gene-targeted embryonic stem cells allowing immediate phenotypic analyses. Nat. Biotechnol. *25*, 91–99.
43. Valenzuela, D.M., Murphy, A.J., Frendewey, D., Gale, N.W., Economides, A.N., Auerbach, W., Poueymirou, W.T., Adams, N.C., Rojas, J., Yasenchak, J., et al. (2003). High-throughput engineering of the mouse genome coupled with high-resolution expression analysis. Nat. Biotechnol. *21*, 652–659.
44. Wood, A.R., Esko, T., Yang, J., Vedantam, S., Pers, T.H., Gustafsson, S., Chu, A.Y., Estrada, K., Luan, J., Kutalik, Z., et al.; Electronic Medical Records and Genomics (eMEMERGEGE) Consortium; MIGen Consortium; PAGEGE Consortium; and LifeLines Cohort Study (2014). Defining the role of common variation in the genomic and biological architecture of adult human height. Nat. Genet. *46*, 1173–1186.
45. Jee, Y.H., Andrade, A.C., Baron, J., and Nilsson, O. (2017). Genetics of Short Stature. Endocrinol. Metab. Clin. North Am. *46*, 259–281.
46. Benko, S., Fantes, J.A., Amiel, J., Kleinjan, D.J., Thomas, S., Ramsay, J., Jamshidi, N., Essafi, A., Heaney, S., Gordon, C.T., et al. (2009). Highly conserved non-coding elements on either side of SOX9 associated with Pierre Robin sequence. Nat. Genet. *41*, 359–364.
47. Liu, X., Gao, L., Zhao, A., Zhang, R., Ji, B., Wang, L., Zheng, Y., Zeng, B., Valenzuela, R.K., He, L., and Ma, J. (2014). Identification of duplication downstream of BMP2 in a Chinese family with brachydactyly type A2 (BDA2). PLoS ONE *9*, e94201.
48. Simpson, A.H., Mills, L., and Noble, B. (2006). The role of growth factors and related agents in accelerating fracture healing. J. Bone Joint Surg. Br. *88*, 701–705.
49. Sonnet, C., Simpson, C.L., Olabisi, R.M., Sullivan, K., Lazard, Z., Gugala, Z., Peroni, J.F., Weh, J.M., Davis, A.R., West, J.L., and Olmsted-Davis, E.A. (2013). Rapid healing of femoral defects in rats with low dose sustained BMP2 expression from PEGDA hydrogel microspheres. J. Orthop. Res. *31*, 1597–1604.
50. Ma, L., Lu, M.F., Schwartz, R.J., and Martin, J.F. (2005). Bmp2 is essential for cardiac cushion epithelial-mesenchymal transition and myocardial patterning. Development *132*, 5601–5611.
51. Li, F.F., Deng, X., Zhou, J., Yan, P., Zhao, E.Y., and Liu, S.L. (2016). Characterization of human bone morphogenetic protein gene variants for possible roles in congenital heart disease. Mol. Med. Rep. *14*, 1459–1464.